

## MODELING ASTROPHYSICAL PLASMAS

CHRISTOPHER W. CHURCHILL<sup>1</sup> AND ELIZABETH KLIMEK<sup>1</sup>

*Draft December 2011*

### ABSTRACT

The physical modeling of the ionization balance of optically thin plasmas are presented. The model assumes ionization equilibrium, and treats photoionization, Auger ionization, direct collisional ionization, excitation auto-ionization, charge exchange ionization, two-body radiative recombination, dielectronic recombination, and charge exchange recombination. Ionization and recombinations rate coefficients are computed using the most up-to-date fitting formulae from the literature. The chemical abundances can be modified to account for various astrophysical environments and chemical enrichment patterns. The model can account for species from hydrogen to zinc. The ionizing photon field can be generalized to include the ultraviolet background (UVB), stellar radiation, or a combination of the two. For the UVB at a given redshift, we adopt a Haardt & Madau spectral energy distribution and for the stellar spectral energy distribution we adopt a Starburst99 model for a stellar population defined by its total mass, age, and metallicity. The “cloud model” is defined by the total hydrogen density,  $n_{\text{H}}$ , the equilibrium temperature,  $T$ , and the abundance pattern. The ionizing radiation field is defined by the “cloud” redshift and/or the stellar population mass, age, metallicity, and distance to the “cloud”.

*Subject headings:* quasars: absorption lines

### 1. INTRODUCTION

In gas structures where the optical depth of photons is well below unity, the ionizing radiation field is not in equilibrium with the gas particles. In these cases, and in astrophysical environments where the ionizing radiation permeating a gas structure does not originate local to the structure, the assumptions required for the use of the Boltzman equation and the Saha equation are not met. Thus, a full treatment of the radiation field must be included, since the photoionization processes are not coupled to the collisional ionization and recombination processes.

In this paper, we present a model for determining the ionization balance in optically thin cloud models. In § 2, we describe our notation and introduce the formalism of modeling the ionization balance of a gas. Ionization processes are described in § 3, recombination processes are described in § 4, and charge exchange processes are described in § 5. The rate equations are derived in § 6. In 7, we describe the model, including the construction of the ionizing radiation field, and the zeroth order solution for solving the rate matrix. The rate matrix is defined in § 8. We show applications of the code in § 9, and provide general conclusions in § 10.

### 2. NOTATION AND FORMALISMS

For what follows, we denote the atomic species by the index  $k$ , where  $k$  equals the atomic number, and denote the ionization stage by the index  $j$ , where  $j = 1$  is the neutral stage and  $j = k + 1$  is the fully ionized stage. We assume that all ions and neutral atoms are in their ground state. The number density [ $\text{cm}^{-3}$ ] of ion  $k, j$  is  $n_{k,j}$  and the electron number density is  $n_e$ .

The rate equation,  $dn_{k,j}/dt$ , which quantifies the rate of change in the number of species  $k, j$  per unit volume per unit time is given by

$$\frac{dn_{k,j}}{dt} = (\text{creation rate of } n_{k,j}) - (\text{destruction rate of } n_{k,j}). \quad (1)$$

Clearly, there is a rate equation for each ionization stage for

each atomic species, which taken together form a rate matrix. These creation and destruction rates [ $\text{cm}^{-3} \text{s}^{-1}$ ] are determined by multiplying the rate per unit time,  $R [\text{s}^{-1}]$ , by the density of the initial state particle, i.e.,  $nR$ . For example, in the case of photoionization of  $n_{k,j}$ , the contribution to the destruction rate term is  $n_{k,j}R_{k,j}^{\text{ph}}$ . In the case of recombination of an electron to  $n_{k,j+1}$ , the contribution to the creation rate term of  $n_{k,j}$  is  $n_{k,j+1}R_{k,j+1}^{\text{rec}}$ . Note that all rates are indexed to the initial ion stage.

All collision based rates are determined from the *rate coefficients*, which are in units  $\text{cm}^3 \text{s}^{-1}$ . We denote ionization rate coefficients as  $\alpha_{k,j} [\text{cm}^3 \text{s}^{-1}]$ , recombination rate coefficients as  $\beta_{k,j} [\text{cm}^3 \text{s}^{-1}]$ . We use the convention that ionization rate coefficients are indexed by referencing the initial ion stage  $j$ , whereas, for recombination,  $j$  refers to the final ion stage. That is, for recombination, rate coefficients index the ion towards which recombination proceeds.

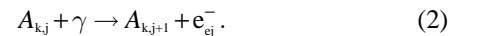
The equilibrium balance is achieved when  $dn_{k,j}/dt = 0$  for all ions, by balancing the creation and destruction rates per unit volume.

### 3. IONIZATION RATES

We treat photoionization, Auger ionization, direct collisional ionization, and excitation auto-ionization processes. We also treat charge exchange ionization, which is presented in § 5.

#### 3.1. Photo and Auger Ionization

Photoionization and Auger ionization both begin with radiative ionization processes. In the case of photoionization, a single electron,  $e_{\text{ej}}^-$ , is ejected and the ionization stage of the incident ion  $k, j$  is incremented by one to  $k, j + 1$ ,



Alternatively, if the incident photon has the required energy, a deep inner shell electron can be liberated and in the process some of its energy can be channelled into also liberating one or more of the less bound, higher shell electrons. This process is known as Auger ionization, in which the ionization stage of

<sup>1</sup> New Mexico State University, MSC 4500, Las Cruces, NM 88003, USA

the incident ion  $k, j$  is incremented by two or more,

$$A_{kj} + \gamma \rightarrow A_{k,m} + (m-j)e_{ej}^-, \quad (3)$$

where we use the convention that the initial ionization stage is  $j$  and the final higher ionization stage is  $m$ . Note that the number of ejected electrons is  $N_e = m - j$ . Because the photo-electron is included in the notation, the final stage  $m$  is always greater than or equal to  $j+2$ . Photoionization is the special case in which  $m = j+1$ .

In order to compute the photo and Auger ionization rates, it is necessary to know the yield probability,  $P_{k,j,m-j}^s$ , i.e., the probability that  $N_e = m - j$  electrons in total are ejected from an ion following a photoionization of an electron originating from shell  $s$  (the photo-electron). These yield probabilities have been calculated and tabulated by Kaastra & Mewe (1993). The convention for the shell indices are  $s = 1$  is the 1s shell,  $s = 2$  is 2s,  $s = 3$  is 2p,  $s = 4$  is 3s,  $s = 5$  is 3p,  $s = 6$  is 3d, and  $s = 7$  is 4s.

For the photo-electron, the total photoionization rate,  $R_{kj}^{\text{ph}}$ , for destruction of ion  $k, j$  is given by  $R_{k,j,s}^{\text{ph}}$  (see Eq. 6), the rate at which an electron bound in shell  $s$  of ion  $k, j$  is ionized by incident photons, weighted by the probability that only the photo-electron is ejected from the ion and summed over all electron shells,

$$R_{kj}^{\text{ph}} = \sum_{s=1}^{N_{kj}^s} P_{k,j,l}^s R_{k,j,s}^{\text{ph}}, \quad (4)$$

where  $N_{kj}^s$  is the number of shells for ion  $k, j$ .

Similarly, the Auger ionization rate,  $R_{k,j,m}^{\text{aug}}$ , for destruction of an ion  $k, j$  that ejects  $N_e = m - j$  electrons (including the photo-electron, so  $N_e \geq 2$ ) is the sum of  $R_{k,j,s}^{\text{ph}}$  over all electron shells weighted by the probability that  $N_e$  electrons in total were ejected from the ion in response to a photo-electron originating in shell  $s$ ,

$$R_{k,j,m}^{\text{aug}} = \sum_{s=1}^{N_{kj}^s} P_{k,j,m-j}^s R_{k,j,s}^{\text{ph}}. \quad (5)$$

Clearly,  $R_{k,k+1,m}^{\text{aug}} = R_{k,k,m}^{\text{aug}} = 0$  since fully ionized and hydrogenic ions cannot undergo Auger ionization.

The rate  $R_{k,j,s}^{\text{ph}}$  depends upon the energy dependent photoionization cross section for that shell,  $\sigma_{k,j,s}^{\text{ph}}(E)$ , where  $E = h\nu$  is the incident photon energy, times the photon number flux per unit frequency,  $4\pi J_\nu / h\nu$  [ $\text{cm}^{-2} \text{s}^{-1} \text{Hz}^{-1}$ ], where  $J_\nu$  is the specific intensity [ $\text{erg cm}^{-2} \text{s}^{-1} \text{sr}^{-1} \text{Hz}^{-1}$ ]. Converting the mean number flux density per unit frequency to the mean number flux density per unit energy, via  $J_E dE = J_\nu d\nu$ , we have

$$R_{k,j,s}^{\text{ph}} = 4\pi \int_{I_{k,j,s}}^{\infty} J_E \sigma_{k,j,s}^{\text{ph}}(E) \frac{dE}{E}, \quad (6)$$

where  $I_{k,j,s}$  is the ionization energy for shell  $s$  of ion  $k, j$ . Calculation of  $J_E$  is described in § 7.3.

For the computation of Eq. 6, the photoionization cross sections are computed from the fitting functions and fitting parameters tabulated by Verner & Iakovlev (1995) for inner shells and by Verner et al. (1996) for the outer shells. Their work includes all ionization stages and shells for hydrogen through zinc. We computed  $\sigma_{k,j,s}^{\text{ph}}(E)$  from,

$$\sigma_{k,j,s}^{\text{ph}}(E) = \sigma_0 y^{-Q} \frac{(x-1)^2 + y_w^2}{[1 + (y/y_A)^{1/2}]^P}, \quad (7)$$

where  $x = E/E_0 - y_0$  and  $y = (x^2 + y_1^2)^{1/2}$ . The tabulated fitting

parameters for each  $k, j, s$  are  $\sigma_0, E_0, y_A, P, y_w, y_0$ , and  $y_1$ . For inner shells  $y_w, y_0$ , and  $y_1$  are null and the asymptotic power is  $Q = \frac{1}{2}P + \ell + \frac{11}{2}$ , where  $\ell$  is the angular momentum quantum number of the shell. For the outer shell  $Q = \frac{1}{2}P + \frac{11}{2}$ . The physical interpretation of each fitting parameter is explained in Verner et al. (1996).

### 3.2. Direct Collisional Ionization

Direct collisional ionization is the collision of an electron with an ion, which then directly ionizes from  $j$  to  $j+1$ . In the process, the colliding free electron,  $e_f^-$ , loses an energy equal to the ionization energy plus the kinetic energy of the ejected electron,

$$A_{kj} + e_f^- \rightarrow A_{k,j+1} + e_f^- + e_{ej}^-. \quad (8)$$

The ionization rate for destruction of ion  $k, j$  due to direct collisional ionization is obtained by multiplying the total direct collisional ionization rate coefficient,  $\alpha_{k,j}^{\text{cdi}}(T)$ , by the number density of free electrons,

$$R_{kj}^{\text{cdi}}(T) = n_e \alpha_{k,j}^{\text{cdi}}(T), \quad (9)$$

where

$$\alpha_{k,j}^{\text{cdi}}(T) = \sum_{s=1}^{N_{kj}^s} \alpha_{k,j,s}^{\text{cdi}}(T). \quad (10)$$

is the sum of the direct collisional ionization rate coefficient contributions,  $\alpha_{k,j,s}^{\text{cdi}}(T)$ , for ejection of an electron from shell  $s$ .

The  $\alpha_{k,j,s}^{\text{cdi}}(T)$  are the expectation values  $\langle \sigma_{k,j,s}^{\text{cdi}} \cdot v \rangle$ , where  $\sigma_{k,j,s}^{\text{cdi}}(E)$  is the direct collisional ionization cross section for the shell,  $v(E) = \sqrt{2kE/m_e}$  is the electron speed for kinetic energy  $E$ , and  $m_e$  is the electron mass. The integration is over energies large enough to overcome the binding energy,

$$\begin{aligned} \alpha_{k,j,s}^{\text{cdi}}(T) &= \langle \sigma_{k,j,s}^{\text{cdi}} \cdot v \rangle \\ &= \sqrt{\frac{2k}{m_e}} \int_{I_{k,j,s}}^{\infty} \sigma_{k,j,s}^{\text{cdi}}(E) f(E, T) E^{1/2} dE, \end{aligned} \quad (11)$$

where  $f(E, T)$  is the Maxwell-Boltzmann speed distribution function at equilibrium temperature  $T$ , and  $I_{k,j,s}$  is the ionization energy of shell  $s$  of ion  $k, j$ .

The direct collisional ionization cross sections and rate coefficients are computed from the fitting functions and parameters tabulated by Arnaud & Rothenflug (1985). For shell  $s$  of ion  $k, j$ , let  $u_1 = E/I_{k,j,s}$  and  $u_2 = 1 - I_{k,j,s}/E$ . The direct collisional ionization cross section for shell  $s$  is computed from

$$\sigma_{k,j,s}^{\text{cdi}}(E) = \frac{10^{-14}}{u_1 I_{k,j,s}^2} \left\{ a_{kj}^s u_2 + b_{kj}^s u_2^2 + c_{kj}^s \ln u_1 + d_{kj}^s \frac{\ln u_1}{u_1} \right\}, \quad (12)$$

where the four fitting coefficients,  $a_{kj}^s, b_{kj}^s, c_{kj}^s$ , and  $d_{kj}^s$ , are tabulated in Arnaud & Rothenflug (1985) for each shell for all ion stages of hydrogen through nickel. The units of the fitting coefficients are  $10^{-14} \text{cm}^2 \text{eV}^2$ .

Rather than integrate Eq. 11 using Eq. 12, which can be computationally expensive, we computed  $\alpha_{k,j,s}^{\text{cdi}}(T)$  for each shell using the fitting formulae of Arnaud & Rothenflug (1985), for which the same fitting coefficients employed for the cross sections apply. Let  $x_{kj}^s = I_{k,j,s}/kT$ , then

$$\alpha_{k,j,s}^{\text{cdi}}(T) = \frac{6.69 \times 10^{-7}}{(kT)^{3/2}} F_{kj}^s(x_{kj}^s) \frac{\exp\{-x_{kj}^s\}}{x_{kj}^s}, \quad (13)$$

where

$$F_{kj}^s(x) = a_{kj}^s [1 - x f_1(x)] + b_{kj}^s [1 + x - x(2+x) f_1(x)] + c_{kj}^s f_1(x) + d_{kj}^s x f_2(x) \quad (14)$$

and where

$$f_1(x) = e^x \int_1^\infty \frac{dt}{t} e^{-xt} \quad f_2(x) = e^x \int_1^\infty \frac{dt}{t} e^{-xt} \ln t. \quad (15)$$

The integral for  $f_1(x)$  is the well known Exponential function. Both  $f_1(x)$  and  $f_2(x)$  are computed from the closed form formulae given in Arnaud & Rothenflug (1985), incorporating the corrections given by Verner & Iakovlev (1990). We then compute the total direct collisional ionization rate coefficient,  $\alpha_{kj}^{\text{cdi}}(T)$ , for ion  $k, j$  using Eq. 10. We also examined the rate coefficient formulae and parameters of Voronov (1997), but found the results comparable.

### 3.3. Excitation-Auto Ionization

Excitation auto-ionization (E-A) occurs in ions with many inner filled shell electrons and only a few outer shell electrons. A collision with a free electron first excites the ion. Then, during the internal deexcitation process the released energy can either channel into recombination emission lines or into liberating an outer shell electron, which is auto-ionization,

$$A_{kj} + e_f^- \rightarrow A_{kj}^* + e_f^- \rightarrow A_{kj+1} + e_{ej}^- + e_f^-, \quad (16)$$

where  $e_f^-$  the free collisional electron and the  $e_{ej}^-$  is ejected auto-ionized electron.

The ionization rate for destruction of ion  $k, j$  due to E-A collisional ionization is obtained by multiplying the E-A collisional ionization rate coefficient,  $\alpha_{kj}^{\text{cea}}(T)$ , by the number density of free electrons,

$$R_{kj}^{\text{cdi}}(T) = n_e \alpha_{kj}^{\text{cea}}(T). \quad (17)$$

The total E-A rate coefficient is given by the expectation value  $\alpha_{kj}^{\text{cea}}(T) = \langle \sigma_{kj}^{\text{cea}} \cdot v \rangle$  computed from Eq. 11 with  $I_{k,j,s}$  replaced by  $\chi_{k,j}$ , the E-A onset energy and  $\sigma_{k,j,s}^{\text{cdi}}(E)$  replaced by  $\sigma_{k,j}^{\text{cdi}}(E)$ , the total E-A cross section, which is obtained by weighting the deexcitation transition channels over all transitions.

The E-A cross sections and rate coefficients depend on the bound electron configuration of the ion, i.e., the isoelectronic sequence. For example,  $\text{C}^{+3}$ ,  $\text{N}^{+4}$ , and  $\text{O}^{+6}$  all have the electron configuration of neutral lithium ( $1s^2 2s$ ) and are thus lithium isoequence ions ( $N_e = 3$ ).

There is no E-A process for hydrogen and helium sequence ions. For lithium sequence ions, the dominant contribution to the cross section is the  $1s-2p$  transition. As the charge of the ion,  $Z$ , increases, the branching ratio to E-A decreases. No significant E-A contribution to the direct collisional cross section is observed for the beryllium sequence (except perhaps  $\text{O}^{+4}$ , which is neglected), nor for the sequences from boron to neon, which differ only in the number of  $2p$  shell electrons. For the sodium sequence ( $[\text{Ne}]3s^1$ ), up to 18 transitions can contribute to E-A, for which the relative importance increases with  $Z$ . The sequences from magnesium to argon differ in the number of  $3p$  shell electrons, and the relative importance of E-A decreases as the shell fills.

We computed the total E-A cross sections and rate coefficients for ions up to nickel using the fitting functions and parameters proposed by Arnaud & Rothenflug (1985), with the exceptions of the iron ions, which are computed from the

fitting functions and parameters updated by Arnaud & Raymond (1992), and the cross sections for the lithium sequence, which we obtained from Hu et al. (1996).

In order to simplify the individually presented fitting functions of Arnaud & Rothenflug (1985) and Hu et al. (1996), we present uniformly generalized fitting functions for which we have distilled several of the their fitting parameters into fewer terms. For ion  $k, j$ , the total E-A cross section is computed from

$$\sigma_{kj}^{\text{cea}}(E) = \frac{\sigma_0}{Z_{\text{eff}}^2} \frac{1}{u_{kj}^a} \left( 1 - \frac{1}{u_{kj}^n} \right), \quad (18)$$

where  $u_{kj} = E/\chi_{k,j}$ , and where  $E$  is the incident electron kinetic energy. The range of applicable  $Z$ , and the fitting parameters,  $\chi_{k,j}$ ,  $Z_{\text{eff}}$ ,  $\sigma_0$ ,  $a$ , and  $n$  are listed in upper panel of Table 1 as a function of isoelectronic sequence, given by  $N_e$ . The translation between isoelectronic sequence and the ion index  $k, j$  is given by  $N_e = k - j + 1$ . Four special cases are treated, for which the fitting function takes the form

$$\sigma_{kj}^{\text{cea}}(E) = \frac{\sigma_0}{u_{kj}} (1 - a \ln u_{kj}), \quad (19)$$

and for which the fitting parameters are listed in the lower panel of Table 1.

For ion  $k, j$ , the total E-A rate coefficients are computed from

$$\alpha_{kj}^{\text{cea}}(T) = \frac{\alpha_0}{Z_{\text{eff}}^2 (1+b)} \frac{G_{\text{iso}}(x_{kj})}{(kT)^{1/2}} \exp\{-x_{kj}\}, \quad (20)$$

where  $x_{kj} = \chi_{k,j}/kT$ , and

$$G_{\text{iso}}(x) = \sum_{n=0}^3 a_n x^n + f_1(x) \sum_{n=0}^3 a_{n+4} x^n, \quad (21)$$

where  $f_1(x)$  is given by Eq. 15. The fitting parameters,  $Z_{\text{eff}}$ ,  $\alpha_0$ ,  $b$ , and coefficients  $a_n$  for  $G_{\text{iso}}(x)$  are listed in the upper panel of Table 2. Note that the range of applicable  $Z$  and the ionization potentials used in Eq. 20 are listed in Table 1.

### 3.4. The Total Collisional Ionization Rate

The E-A process contributes to the direct collisional ionization process such that the total collisional ionization rate for destruction of ion  $k, j$  due to direct ionization and E-A is obtained by adding the respective rates,

$$R_{kj}^{\text{coll}}(T) = R_{kj}^{\text{cdi}}(T) + R_{kj}^{\text{cea}}(T) = n_e [\alpha_{kj}^{\text{cdi}}(T) + \alpha_{kj}^{\text{cea}}(T)]. \quad (22)$$

## 4. RECOMBINATION RATES

We treat radiative recombination and dielectronic recombination processes. Charge exchange recombination is discussed in § 5

### 4.1. Radiative Recombination

Radiative recombination is the capture of a free electron by ion  $k, j+1$  followed by the emission of a photon,

$$A_{kj+1} + e_f^- \rightarrow A_{kj} + \gamma. \quad (23)$$

The radiative recombination rate for creation of ion  $k, j$  due to electron recombination with ion  $k, j+1$  is obtained by multiplying the total recombination rate coefficient,  $\beta_{kj}^{\text{ph}}(T)$ , by the electron number density,

$$R_{kj+1}^{\text{ph}}(T) = n_e \beta_{kj}^{\text{ph}}(T). \quad (24)$$

TABLE 1  
FITTING PARAMETERS FOR EXCITATION-AUTOIONIZATION CROSS SECTIONS<sup>a</sup>

Sequence	$N_e$	Z Range	$\chi_{k,j}$ [eV]	$Z_{\text{eff}}$	$\sigma_0$ [cm <sup>2</sup> ]	$a$	$n$
[He]2s <sup>1</sup> Li <sup>b</sup>	3	4–28	$13.6 \{(Z-0.835)^2 + (Z-1.62)^2\}$	$Z^2$	$4.22 \times 10^{-16}$	1/3	20
[Ne]3s <sup>1</sup> Na (low Z)	11	12–16	$26.0(Z-10)$	$(Z-11)^{0.35}$	$2.8 \times 10^{-17}$	1	1
[Ne]3s <sup>1</sup> Na (high Z)	11	18–28	$11.0(Z-10)^{1.50}$	$(Z-10)^{1.87}$	$1.3 \times 10^{-14}$	1	3
[Ne]3s <sup>2</sup> Mg	12	18–28	$10.3(Z-10)^{1.52}$	$Z$	$4.0 \times 10^{-13}/\chi_{k,j}$	1	3
[Ne]3p <sup>1</sup> Al	13	18–28	$18.0(Z-11)^{1.33}$	$Z$	$4.0 \times 10^{-13}/\chi_{k,j}$	1	3
[Ne]3p <sup>2</sup> Si	14	18–28	$18.4(Z-12)^{1.36}$	$Z$	$4.0 \times 10^{-13}/\chi_{k,j}$	1	3
[Ne]3p <sup>3</sup> P	15	18–28	$23.7(Z-13)^{1.29}$	$Z$	$4.0 \times 10^{-13}/\chi_{k,j}$	1	3
[Ne]3p <sup>4</sup> S	16	18–28	$40.0(Z-14)^{1.10}$	$Z$	$4.0 \times 10^{-13}/\chi_{k,j}$	1	3
Special Cases							
[Ar]4s <sup>2</sup> Ca <sup>0</sup>	20	20	25.0	...	$6.0 \times 10^{-17}$	1.12	...
[Ar]4s <sup>1</sup> Ca <sup>+1</sup>	19	20	29.0	...	$9.8 \times 10^{-17}$	1.12	...
[Ar]3d <sup>3</sup> 4s <sup>2</sup> Fe <sup>+3</sup>	23	26	60.0	...	$1.8 \times 10^{-17}$	1.0	...
[Ar]3d <sup>2</sup> 4s <sup>2</sup> Fe <sup>+4</sup>	22	26	73.0	...	$5.0 \times 10^{-18}$	1.0	...

<sup>a</sup> The connection between isoelectronic series and index  $k, j$  is  $N_e = k - j + 1$  and  $Z = k$ .

<sup>b</sup> The fitting parameters for lithium are taken from Hu et al. (1996).

TABLE 2  
FITTING PARAMETERS FOR EXCITATION-AUTOIONIZATION RATE COEFFICIENTS<sup>a</sup>

Sequence	$Z_{\text{eff}}$	$\alpha_0$ [cm <sup>3</sup> s <sup>-1</sup> eV <sup>1/2</sup> ]	$b$	$G_{\text{iso}}(x) : a_0; a_1; a_2; a_3; a_4; a_5; a_6; a_7$
[He]2s <sup>1</sup> Li <sup>b</sup>	$(Z-0.43)$	$1.600 \times 10^{-7}$	0.0002Z <sup>3</sup>	0.67; 1.20; 0; 0; 2.22; -0.18; -1.20; 0
[Ne]3s <sup>1</sup> Na (low Z)	$(Z-11)^{0.35}$	$1.873 \times 10^{-9}/\chi_{k,j}$	0	1.00; 0; 0; 0; 0; -1.00; 0; 0
[Ne]3s <sup>1</sup> Na (high Z)	$(Z-10)^{1.87}$	$8.697 \times 10^{-7}/\chi_{k,j}$	0	1.00; -0.50; 0.50; 0; 0; 0; 0; -0.50
[Ne]3s <sup>2</sup> Mg	$Z$	$2.676 \times 10^{-5}$	0	1.00; -0.50; 0.50; 0; 0; 0; 0; -0.50
[Ne]3p <sup>1</sup> Al	$Z$	$2.676 \times 10^{-5}$	0	1.00; -0.50; 0.50; 0; 0; 0; 0; -0.50
[Ne]3p <sup>2</sup> Si	$Z$	$2.676 \times 10^{-5}$	0	1.00; -0.50; 0.50; 0; 0; 0; 0; -0.50
[Ne]3p <sup>3</sup> P	$Z$	$2.676 \times 10^{-5}$	0	1.00; -0.50; 0.50; 0; 0; 0; 0; -0.50
[Ne]3p <sup>4</sup> S	$Z$	$2.676 \times 10^{-5}$	0	1.00; -0.50; 0.50; 0; 0; 0; 0; -0.50
Special Cases				
[Ar]4s <sup>2</sup> Ca <sup>0</sup>	1.0	$4.014 \times 10^{-9}/\chi_{k,j}$	0	1.00; 0; 0; 0; 1.12; 0; 0; 0
[Ar]4s <sup>1</sup> Ca <sup>+1</sup>	1.0	$6.556 \times 10^{-9}/\chi_{k,j}$	0	1.00; 0; 0; 0; 1.12; 0; 0; 0
[Ar]3d <sup>3</sup> 4s <sup>2</sup> Fe <sup>+3</sup>	1.0	$1.204 \times 10^{-9}/\chi_{k,j}$	0	1.00; 0; 0; 0; 1.00; 0; 0; 0
[Ar]3d <sup>2</sup> 4s <sup>2</sup> Fe <sup>+4</sup>	1.0	$3.345 \times 10^{-9}/\chi_{k,j}$	0	1.00; 0; 0; 0; -1.00; 0; 0; 0

<sup>a</sup> The connection between isoelectronic series and index  $k, j$  is  $N_e = k - j + 1$  and  $Z = k$ .

<sup>b</sup> The tabulated value of  $\alpha_0$  for the lithium sequence requires an additional multiplicative term. For C<sup>+3</sup>, multiply by 0.6. For N<sup>+4</sup>, multiply by 0.8. For O<sup>+5</sup>, multiply by 1.25. For all other ions, multiply by 1.2.

The cross section for capture of a free electron decreases with electron kinetic energy. Given the cross section,  $\sigma_{k,j,s}^{\text{rec}}(E)$ , for radiative recombination to shell  $s$  forming ion  $k, j$ , the radiative recombination rate coefficient for the shell,  $\beta_{k,j,s}^{\text{ph}}(T)$ , is obtained by integrating over all electron velocities, analogous to Eq. 11, i.e., with no threshold energy ( $I_{k,j,s} \rightarrow 0$ ) and with  $\sigma_{k,j,s}^{\text{cdi}}(E)$  replaced by  $\sigma_{k,j,s}^{\text{rec}}(E)$ . We have ignored radiation induced recombination. The total recombination rate coefficient is the sum over all shells,

$$\beta_{k,j}^{\text{ph}}(T) = \sum_{s=1}^{N_{k,j}^s} \beta_{k,j,s}^{\text{ph}}(T). \quad (25)$$

For hydrogenic ions ( $N_e = 1$ ) we use the formula originally proposed by Seaton (1959), which remains the most accurate (Arnaud & Rothenflug 1985; Dopita & Sutherland 2003),

$$\beta_{k,j}^{\text{ph}}(T) = \beta_0 Z_k \lambda^{1/2} [0.4288 + 0.5 \ln \lambda + 0.469 \lambda^{-1/3}], \quad (26)$$

where  $\beta_0 = 5.197 \times 10^{-14}$  and where  $\lambda = Z_k^2 (1.5789 \times 10^5 / T)$ .

The Atomic and Molecular Diagnostic Processes in Plasmas (AMDPP) group has published fitting functions and

parameters for radiative recombination rate coefficients for many non-hydrogenic ions (Badnell 2006). The functional form is

$$\beta_{k,j}^{\text{ph}}(T) = \frac{a_{k,j}}{(T/t_{k,j}^{(0)})^{1/2}} \frac{\left[1 + (T/t_{k,j}^{(0)})^{1/2}\right]^{b'_{k,j}-1}}{\left[1 + (T/t_{k,j}^{(1)})^{1/2}\right]^{b'_{k,j}+1}}, \quad (27)$$

where  $a_{k,j}$ ,  $t_{k,j}^{(0)}$ ,  $t_{k,j}^{(1)}$  are tabulated fitting parameters, and  $b'_{k,j} = b_{k,j} + c_{k,j} \exp\{-t_{k,j}^{(2)}/T\}$ , where  $b_{k,j}$ ,  $c_{k,j}$  and  $t_{k,j}^{(2)}$  are additional fitting parameters. Data are tabulated for all elements from helium to zinc for isoelectronic sequences up to the magnesium sequence ([Ne]3s<sup>2</sup>,  $N_e = 12$ ). The fitting functions neglect narrow resonant spikes.

Since not all ionization stages have been tabulated by Badnell (2006), we employed the fitting functions and parameters for the simple power-law form published by Arnaud & Rothenflug (1985), based upon work of Seaton (1959), Aldrovandi & Pequignot (1973), and Shull & Van Steenberg (1982) for cases omitted from the AMDPP tables. The ex-

pression is

$$\beta_{k,j}^{\text{ph}}(T) = a_{k,j} T_4^{-b_{k,j}}, \quad (28)$$

where  $T_4 = T/10^4$ , and where  $a_{k,j}$  and  $b_{k,j}$  are the fitting parameters tabulated by Arnaud & Rothenflug (1985) for all ions of helium through nickel.

#### 4.2. Dielectronic Recombination

Dielectronic recombination often dominates over radiative recombination. In this process, a high energy free electron first excites a bound deep inner shell electron prior to its capture in an elevated excited state of the ion. There are now two excited electrons and an unfilled state in an inner shell. Multiple channels of relaxation for the ion are now available, including auto-ionization.

In dielectronic recombination, the doubly excited ion works its way back to the ground state via multiple radiative cascades. At high temperatures this process usually proceeds first by the decay of one of the excited electrons to refill the empty inner shell by radiative decay followed by a downward cascade of the remaining excited electron. At low temperatures, the dominant channel occurs when the free electron is captured in a shell that is a resonant state to the emptied inner shell, which decays rapidly and is then followed by a downward cascade of the remaining excited electron. The reaction can be written

$$A_{k,j+1} + e^- \rightarrow A_{k,j}^{**} \rightarrow A_{k,j}^* + \gamma \rightarrow A_{k,j+1} + \sum \gamma_i, \quad (29)$$

where the sum indicates that several recombination photons can be emitted during the cascade process.

The dielectronic recombination rate for creation of ion  $k, j$  due to electron recombination with ion  $k, j+1$  is obtained by multiplying the total dielectronic recombination rate coefficient,  $\beta_{k,j}^{\text{die}}(T)$ , by the electron number density,

$$R_{k,j+1}^{\text{die}}(T) = n_e \beta_{k,j}^{\text{die}}(T). \quad (30)$$

Since the dominant channels for dielectronic recombination are temperature dependent, the rate coefficient is double peaked. For this reason, previous fitting functions and parameters for the rate coefficients were split into a low temperature regime (Nussbaumer & Storey 1983, 1986, 1987) and high temperature regime (Aldrovandi & Pequignot 1973; Shull & Van Steenberg 1982; Arnaud & Rothenflug 1985).

A newer fitting function and accompanying parameter list for all elements from helium to zinc and valid for temperatures ranging from  $T \simeq 100$  to  $T \simeq 10^7$  K has been made available by the AMDPP group. We used the fitting functions and parameters described in Altun et al. (2007), which are based upon a series of papers (see references in Badnell et al. 2003; Altun et al. 2007). The fitting function has the form

$$\beta_{k,j}^{\text{die}}(T) = T^{-3/2} \sum_{i=1}^{N_{k,j}} c_{k,j,i} \exp\left\{-\frac{t_{k,j,i}}{T}\right\}, \quad (31)$$

where  $N_{k,j}$  is the number of fitting parameters for ion  $k, j$ , and  $c_{k,j,i}$  and  $t_{k,j,i}$  are the fitting parameters.

#### 5. CHARGE EXCHANGE

Charge exchange is the transfer of an electron from one ion to another during a collision. Since hydrogen is the most abundant species, a charge exchange with a given metal ion  $k, j$  is dominated either by ionization ( $k, j \rightarrow k, j+1$ ) from an ionized hydrogen (in which the  $\text{H}^+$  ion recombines with the

exchanged electron), or by recombination ( $k, j-1 \rightarrow k, j$ ) via the ionization of neutral hydrogen,

$$A_{k,j} + \text{H}^+ \leftrightarrow A_{k,j+1} + \text{H}^0. \quad (32)$$

Helium is also relatively abundant and is the second most important charge exchange channel,

$$A_{k,j+1} + \text{He}^0 \leftrightarrow A_{k,j} + \text{He}^+. \quad (33)$$

The rate for destruction of ion  $k, j$  via charge exchange ionization with ionized hydrogen ( $k = 1, j = 2$ ) is

$$R_{k,j}^{\text{exH}^+}(T) = n_{1,2} \alpha_{k,j}^{\text{exH}^+}(T), \quad (34)$$

where  $\alpha_{k,j}^{\text{exH}^+}(T)$  is the ionization rate coefficient. The rates for creation of ion  $k, j-1$  via destruction of ion  $k, j$  via charge exchange recombination with neutral hydrogen ( $k = 1, j = 1$ ) and with neutral helium ( $k = 2, j = 1$ ) are given by

$$\begin{aligned} R_{k,j}^{\text{exH}}(T) &= n_{1,1} \beta_{k,j-1}^{\text{exH}}(T) \\ R_{k,j}^{\text{exHe}}(T) &= n_{2,1} \beta_{k,j-1}^{\text{exHe}}(T), \end{aligned} \quad (35)$$

where  $\beta_{k,j-1}^{\text{exH}}(T)$  and  $\beta_{k,j-1}^{\text{exHe}}(T)$  are the respective recombination rate coefficients.

We computed the total charge exchange ionization and recombination rate coefficients using the fitting function and parameters of Kingdon & Ferland (1996). The rate coefficient for recombination to ion  $k, j$  via charge exchange from neutral hydrogen is given by

$$\beta_{k,j}^{\text{exH}}(T) = 10^{-9} a_{k,j} T_4^{b_{k,j}} [1 + c_{k,j} \exp\{d_{k,j} T_4\}], \quad (36)$$

where  $T_4 = T/10^4$ , and where  $a_{k,j}$ ,  $b_{k,j}$ ,  $c_{k,j}$ , and  $d_{k,j}$  are the fitting parameters. The rate coefficient for ionization of ion  $k, j$  via charge exchange to neutral hydrogen is obtained via detailed balancing,

$$\alpha_{k,j}^{\text{exH}^+}(T) = \beta_{k,j}^{\text{exH}}(T) \exp\left\{-\frac{\Delta E_{k,j}}{kT_4}\right\}, \quad (37)$$

where the Boltzmann factor,  $\Delta E_{k,j}/k$ , is also tabulated by Kingdon & Ferland (1996).

The computation of the recombination rate coefficient for charge exchange with neutral helium,  $\beta_{k,j}^{\text{exHe}}(T)$ , is also obtained from Eq. 36 using the parameters for applicable to these reactions. The charge exchange ionization of metals via ionized helium is not treated because, to date, there is not a uniform set of published rates for a covering a wide range of ions.

The fitting parameters provided by Kingdon & Ferland (1996) are presented for all species up to and including zinc, but only for the first three ionization stages. For ions with  $j \geq 4$ , we use the asymptotic formulae of Ferland, Korista, & Verner (1997),

$$\beta_{k,j}^{\text{exH}}(T) = 1.92 \times 10^{-9} Z_k, \quad (38)$$

for hydrogen, and

$$\beta_{k,j}^{\text{exHe}}(T) = 5.4 \times 10^{-10} Z_k, \quad (39)$$

for helium. The different constants are due to the different reduced mass of the ion in terms of the electron mass for hydrogen and helium interactions.

## 6. RATE EQUATIONS

Here, we derive the rate equations,  $dn_{kj}/dt$ , for all ionization stages of all treatable species. We include photoionization, direct collisional ionization, excitation autoionization, radiative recombination, dielectronic recombination, and charge exchange with hydrogen and helium. We assume two-level atoms, effectively the ground state and the continuum<sup>2</sup>.

For the following, we drop the explicit temperature dependence of all rates and rate coefficients. We remind the reader that for recombination, the rate coefficients,  $\beta_{kj}$ , are indexed to the final state. However, we use the convention that all rates,  $R_{kj}$ , are indexed by the initial state.

## 6.1. Hydrogen

Hydrogen is the simplest case because the channels for creation and destruction involve only two adjacent ionization stages. Because of this, the hydrogen rate equations for  $n_{1,1}$  and  $n_{1,2}$  are antisymmetric,

$$\begin{aligned} \frac{dn_{1,1}}{dt} &= n_{1,2} (R_{1,2}^{\text{rec}} + R_{1,2}^{\text{exH}^+}) - n_{1,1} (R_{1,1}^{\text{ph}} + R_{1,1}^{\text{coll}} + R_{1,1}^{\text{exH}}) \\ \frac{dn_{1,2}}{dt} &= -\frac{dn_{1,1}}{dt}. \end{aligned} \quad (40)$$

The creation rates of  $n_{1,1}$  are due to the recombination of  $n_{1,2}$  with free electrons,  $R_{1,2}^{\text{rec}}$ , and ionization charge exchange from metals,  $R_{1,2}^{\text{exH}^+}$ , where

$$\begin{aligned} R_{1,2}^{\text{rec}} &= n_e \beta_{1,1}^{\text{ph}} \\ R_{1,2}^{\text{exH}^+} &= \sum_{k=2}^{\infty} \sum_{j=1}^k n_{k,j} \alpha_{k,j}^{\text{exH}^+}. \end{aligned} \quad (41)$$

The destruction rates of  $n_{1,1}$  are due to photoionization,  $R_{1,1}^{\text{ph}}$ , collisional ionization via free electrons,  $R_{1,1}^{\text{coll}}$ , and recombination charge exchange to metals,  $R_{1,1}^{\text{exH}}$ , which ionizes neutral hydrogen, where

$$\begin{aligned} R_{1,1}^{\text{coll}} &= n_e \alpha_{1,1}^{\text{cdi}} \\ R_{1,1}^{\text{exH}} &= \sum_{k=2}^{\infty} \sum_{j=2}^{k+1} n_{k,j} \beta_{k,j-1}^{\text{exH}}. \end{aligned} \quad (42)$$

Note that the negative of these rates are also the destruction and creation rates of  $n_{1,2}$ , respectively.

## 6.2. Helium

Helium has three ionization stages. There is no published Auger channel directly connecting the neutral and fully ionized stages; however, non-zero dielectronic rate coefficients for the channel from singly ionized to neutral helium exist. The rate equation for neutral helium is

$$\frac{dn_{2,1}}{dt} = n_{2,2} (R_{2,2}^{\text{rec}} + R_{2,2}^{\text{exHe}^+}) - n_{2,1} (R_{2,1}^{\text{ph}} + R_{2,1}^{\text{coll}} + R_{2,1}^{\text{exHe}}). \quad (43)$$

The creation rates of  $n_{2,1}$  are due to the recombination channels of  $n_{2,2}$  with free electrons,  $R_{2,2}^{\text{rec}}$ , and ionization charge exchange

from metals,  $R_{2,2}^{\text{exHe}^+}$ , where

$$\begin{aligned} R_{2,2}^{\text{rec}} &= n_e (\beta_{2,1}^{\text{ph}} + \beta_{2,1}^{\text{die}}) \\ R_{2,2}^{\text{exHe}^+} &= n_{1,1} \alpha_{1,1}^{\text{exHe}^+} + \sum_{k=3}^{\infty} \sum_{j=1}^k n_{k,j} \alpha_{k,j}^{\text{exHe}^+}. \end{aligned} \quad (44)$$

Recall, however, that we do not treat charge exchange ionization from ionized helium, so  $R_{2,2}^{\text{exHe}^+} = 0$  for our work.

The destruction rates of  $n_{2,1}$  are due to photoionization,  $R_{2,1}^{\text{ph}}$ , collisional ionization via free electrons,  $R_{2,1}^{\text{coll}}$ , and recombination charge exchange to metals,  $R_{2,1}^{\text{exH}}$ , which singly ionizes neutral helium, where

$$\begin{aligned} R_{2,1}^{\text{coll}} &= n_e \alpha_{2,1}^{\text{cdi}} \\ R_{2,1}^{\text{exH}} &= n_{1,2} \beta_{1,1}^{\text{exH}} + \sum_{k=3}^{\infty} \sum_{j=2}^{k+1} n_{k,j} \beta_{k,j-1}^{\text{exH}}, \end{aligned} \quad (45)$$

respectively. For twice ionized helium, the rate equation is

$$\frac{dn_{2,3}}{dt} = n_{2,2} (R_{2,2}^{\text{ph}} + R_{2,2}^{\text{coll}} + R_{2,2}^{\text{exH}^+}) - n_{2,3} (R_{2,3}^{\text{rec}} + R_{2,3}^{\text{exH}}). \quad (46)$$

The creation rates via the destruction of  $n_{2,2}$  are due to photoionization,  $R_{2,2}^{\text{ph}}$ , collisional ionization,  $R_{2,2}^{\text{coll}}$ , and ionization via charge exchange recombination to ionized hydrogen, where

$$\begin{aligned} R_{2,2}^{\text{coll}} &= n_e \alpha_{2,2}^{\text{cdi}} \\ R_{2,2}^{\text{exH}^+} &= n_{1,2} \alpha_{2,2}^{\text{exH}^+}. \end{aligned} \quad (47)$$

The destruction rates of  $n_{2,3}$  are due to the channels of recombination with free electrons,  $R_{2,3}^{\text{rec}}$ , and recombination via charge exchange ionization of neutral hydrogen, where

$$\begin{aligned} R_{2,3}^{\text{rec}} &= n_e \beta_{2,3}^{\text{ph}} \\ R_{2,3}^{\text{exH}} &= n_{1,1} \beta_{2,2}^{\text{exH}}. \end{aligned} \quad (48)$$

For singly ionized helium, the creation and destruction rates are simply the negative of the sum of those for neutral and doubly ionized helium,

$$\frac{dn_{2,2}}{dt} = - \left( \frac{dn_{2,1}}{dt} + \frac{dn_{2,3}}{dt} \right). \quad (49)$$

## 6.3. Metals

The general rate equation for the equilibrium density of ion  $n_{k,j}$ , where  $k > 2$ , is easily visualized if one considers the creation and destruction channels from adjacent ionization stages separately from the Auger ionization channels. For what follows, let  $R_{k,j-1}^{\text{ion}}$  denote the creation rate of  $n_{k,j}$  via ionization of  $n_{k,j-1}$  and let  $R_{k,j+1}^{\text{rec}}$  denote the creation rate of  $n_{k,j}$  via recombination from initial state  $n_{k,j+1}$ . Further, let  $R_{k,j}^{\text{rec}}$  denote the destruction rate of  $n_{k,j}$  via recombination to final state  $n_{k,j-1}$  and let  $R_{k,j}^{\text{ion}}$  denote the destruction of  $n_{k,j}$  via ionization to final state  $n_{k,j+1}$ . We then write

$$\begin{aligned} \frac{dn_{k,j}}{dt} &= n_{k,j-1} R_{k,j-1}^{\text{ion}} + n_{k,j+1} R_{k,j+1}^{\text{rec}} + \sum_{i=1}^{j-2} n_{k,i} R_{k,i,j}^{\text{aug}} \\ &\quad - n_{k,j} \left( R_{k,j}^{\text{ion}} + R_{k,j}^{\text{rec}} + \sum_{m=j+2}^{k-1} R_{k,j,m}^{\text{aug}} \right). \end{aligned} \quad (50)$$

The creation rate of  $n_{k,j}$  via ionization destruction of adjacent ion  $n_{k,j-1}$  is

$$R_{k,j-1}^{\text{ion}} = R_{k,j-1}^{\text{ph}} + n_e (\alpha_{k,j-1}^{\text{cdi}} + \alpha_{k,j-1}^{\text{cea}}) + n_{1,2} \alpha_{k,j-1}^{\text{exH}^+}. \quad (51)$$

<sup>2</sup> For a brief discussion of the ramification of this assumption, see § 11.1 of *Hazy 2* (Ferland 2002).

Note that we do not treat charge exchange ionization from ionized helium. The creation rate of  $n_{kj}$  via recombination destruction of adjacent ion  $n_{k,j+1}$  is

$$R_{k,j+1}^{\text{rec}} = n_e (\beta_{k,j}^{\text{ph}} + \beta_{k,j}^{\text{die}}) + n_{1,1} \beta_{k,j}^{\text{exH}} + n_{2,1} \beta_{k,j}^{\text{exHe}}. \quad (52)$$

The recombination destruction rate of  $n_{kj}$  to adjacent stage  $n_{k,j-1}$  and the ionization destruction rate of  $n_{kj}$  to adjacent stage  $n_{k,j+1}$ , are

$$R_{kj}^{\text{rec}} = n_e (\beta_{k,j-1}^{\text{ph}} + \beta_{k,j-1}^{\text{die}}) + n_{1,1} \beta_{k,j-1}^{\text{exH}} + n_{2,1} \beta_{k,j-1}^{\text{exHe}} \quad (53)$$

$$R_{kj}^{\text{ion}} = R_{kj}^{\text{ph}} + n_e (\alpha_{k,j}^{\text{cdi}} + \alpha_{k,j}^{\text{cea}}) + n_{1,2} \alpha_{k,j}^{\text{exH}^+},$$

respectively. The summation terms in Eq. 50 account for Auger ionization processes, which skip adjacent ionization stages. All ions of species  $k$  from the neutral stage to ionization stage  $i \leq j-2$  can contribute to the creation rate of  $n_{kj}$  due to their destruction via Auger ionization

$$\left. \frac{dn_{kj}}{dt} \right|_{\text{aug}} = \sum_{i=1}^{j-2} n_{k,i} R_{k,i,j}^{\text{aug}}. \quad (54)$$

Similarly, ion  $k, j$  can be destroyed by Auger ionization to high ionization final stage  $m$ , where  $m \geq j+2$ ,

$$\left. \frac{dn_{kj}}{dt} \right|_{\text{aug}} = -n_{kj} \sum_{m=j+2}^{k-1} R_{k,j,m}^{\text{aug}}. \quad (55)$$

In practice, Auger ionization is a viable creation and destruction channel only for  $k \geq 4$ .

## 7. THE MODEL

The goal of the model is to calculate the equilibrium number densities,  $n_{k,j}$ . The model requires as input (1) the total hydrogen density of the cloud,  $n_{\text{H}} \equiv n_1$ , (2) the equilibrium temperature of the cloud,  $T$ , (3) the selected metals to be treated [hydrogen and helium are always treated], which defines  $N_k$ , the number of species included, (4) the mass fraction of metals in solar units,  $Z_{\text{cl}}/Z_{\odot}$ , (5) the logarithmic factors by which the abundance of a given species departs from its solar abundance fraction,  $\epsilon_k$ , and (6) the source(s) of the ionizing spectrum,  $J_{\nu}$ .

The options for  $J_{\nu}$  are the ultraviolet background, in which case the redshift of the cloud,  $z_{\text{cl}}$  is required, and/or a stellar population, in which case the properties of the population and its distance to the cloud are required (see § 7.3).

Following the computation of an initial zeroth-order solution (see § 7.4), the final equilibrium solution is obtained by solving the rate matrix using the non-linear least-squares minimization routine DNLS1 (More 1977), which is a modified Levenberg-Marquardt algorithm. The output of the code are the ionization and recombination rate coefficients, ionization fractions, and number densities for all ionic species, as well as the electron density.

### 7.1. Particle and Charge Conservation

Particle conservation is given by

$$n_{\text{tot}} = n_{\text{A}} + n_{\text{e}} = \sum_{k=1}^{N_k} n_k + n_{\text{e}}, \quad n_k = \eta_k n_{\text{A}} = \sum_{j=1}^{k+1} n_{k,j}, \quad (56)$$

where  $n_{\text{A}}$  is the number density of all atomic species, and  $\eta_k$  is the abundance fraction of species  $k$ . The  $n_k$  are constrained to the input hydrogen number density by  $n_{\text{A}} = n_{\text{H}}/\eta_{\text{H}}$ , where  $\eta_{\text{H}} \equiv \eta_1$ .

The  $\eta_k$  are determined by scaling the solar mass fractions,  $(x_k/x_{\text{H}})_{\odot}$ , which are defined as the ratio of the mass fraction of species  $k$  to the mass fraction of hydrogen. We employ the values tabulated in Table 1.4 of Draine (2011) for hydrogen through zinc ( $k = 30$ ), which are determined from the solar abundances tabulated by Asplund et al. (2009). For nonzero  $\epsilon_k$ , we first scale the mass fraction according to  $x_k/x_{\text{H}} = (x_k/x_{\text{H}})_{\odot} \cdot 10^{\epsilon_k}$ . The final scaling to obtain  $\eta_k$  for each of the  $N_k$  species included in a cloud model conserves the total mass fraction of metals to be  $Z_{\text{cl}}/Z_{\odot}$ .

Since each ion  $k, j$  donates  $N_{\text{e}} = j-1$  electrons to the free electron pool, charge conservation dictates

$$n_{\text{e}} = \sum_k \sum_{j=2}^{k+1} (j-1) n_{k,j} = n_{\text{A}} \sum_k \eta_k \sum_{j=2}^{k+1} (j-1) f_{k,j}(n_{\text{e}}, T, J_E), \quad (57)$$

where  $f_{k,j}(n_{\text{e}}, T, J_E) = n_{k,j}/n_k$  is the ionization fraction of ion  $k, j$ . Charge conservation provides the constraint equation in the rate matrix (see § 8). Since  $n_{\text{e}}$  appears in the collisional ionization and recombination rates, and the ionization fractions depend upon  $n_{\text{e}}$ , we immediately see the non-linear aspect of solving for the equilibrium number densities.

### 7.2. Condition of Validity

Because we do not treat radiative transfer through the cloud itself, the model is appropriate only for optically thin gas (also see Verner & Iakovlev 1990). If we use the criterion that the optical depth at the Lyman edge is less than unity, then  $N(\text{H I}) \leq 2 \times 10^{17} \text{ cm}^2$  is the upper limit of validity. Assuming  $D_{\text{cl}} = N(\text{H I})/(f_{\text{H}} n_{\text{H}})$ , we obtain the upper limit of validity on the cloud size to be  $D_{\text{cl}} \leq 650 \cdot (0.01/f_{\text{H}}) \cdot (0.01/n_{\text{H}}) \text{ pc}$ , where  $f_{\text{H}} = f_{1,1} = n_{1,1}/n_1$ .

### 7.3. Ionizing Spectrum

The spectral energy distribution (SED) of the ionizing radiation is employed in Eq. 6 to compute  $R_{k,j,s}^{\text{ph}}$ , the rate at which an electron bound in shell  $s$  of ion  $k, j$  is ionized by incident photons. We provide for the options (1) ionization by the ultraviolet background (UVB), which is redshift dependent, (2) ionization by a stellar population, which depends upon the total stellar mass, age of the population, metallicity of the population, and the distance from the model cloud to the stellar population, and (3) ionization by a combined UVB and a stellar population SED.

For the UVB, we use the SEDs of Haardt & Madau (2011) added to the cosmic microwave background. These spectra are specified as the specific intensity,  $J_{\nu}$  [ $\text{erg s}^{-1} \text{ cm}^{-2} \text{ str}^{-1} \text{ Hz}^{-1}$ ] over the energy [eV] interval  $-6.7 \leq \log E \leq 6.8$  and are provided for redshifts  $0 \leq z \leq 5$ . Once the cloud redshift is specified, a grid of SEDs sampled at intervals of  $\Delta z = 0.2$  are cubic spline interpolated at each frequency to obtain  $J_{\nu}(z_{\text{cl}})$ , which is then converted to the specific intensity per unit energy,  $J_E(z_{\text{cl}})$  versus  $E$  [ $\text{cm}^{-1} \text{ s}^{-1} \text{ str}^{-1}$  vs. eV].

For the stellar populations, we use SEDs computed from the Starburst99 v6.02 models (Sb99, Leitherer et al. 1999). We built a library of SEDs comprising stellar populations of  $M = 10^3, 10^4, 10^5$ , and  $10^6 M_{\odot}$ . For each mass, five ages were computed (1, 5, 10, 20, and 40 Myr) and for each mass and age five metallicities were computed ( $10^{-4}, 10^{-3}, 10^{-2}, 10^{-1}$ , and  $1 Z_{\odot}$ ). We store the SEDs as the luminosity density per unit wavelength,  $L_{\lambda}$  [ $\text{erg s}^{-1} \text{ \AA}$ ] over the wavelength range  $91 \leq \lambda \leq 1.6 \times 10^6 \text{ \AA}$ , which corresponds to the energy [eV] interval  $-2.1 \leq \log E \leq 2.1$ .

Once the desired mass, age, and metallicity are specified, we first cubic spline interpolate  $L_\lambda$  at each wavelength across mass for each age and metallicity, then across age for each metallicity, and then across metallicity. The final SED is then converted to the flux density per unit wavelength,  $F_\lambda = L_\lambda / (4\pi r^2)$  [erg s<sup>-1</sup> cm<sup>-2</sup> str<sup>-1</sup> Å<sup>-1</sup>], where  $r$  is the specified distance to the stellar population from the model cloud. Finally, we convert the SED to  $J_E$  versus  $E$  [cm<sup>-1</sup> s<sup>-1</sup> str<sup>-1</sup> vs. eV].

If a combined UVB plus Sb99 SED is used, the two specific intensities are added. In general, the contribution by stars scales linearly with the mass of the stellar population and with the inverse square of the distance between the model cloud and the stellar population.

#### 7.4. Zeroth Order Solution

An initial guess solution for the density of each ionic species is obtained assuming ionization and recombination balance of adjacent ion stages. Setting  $dn_{k,j}/dt = 0$ , and neglecting Auger ionization, Eq. 50 yields

$$n_{k,j-1}R_{k,j-1}^{\text{ion}} + n_{k,j+1}R_{k,j+1}^{\text{rec}} = n_{k,j}(R_{k,j}^{\text{ion}} + R_{k,j}^{\text{rec}}). \quad (58)$$

If we further neglect charge exchange and coupling of  $n_{k,j}$  with  $n_{k,j-1}$ , we obtain

$$\Phi_{k,j}(n_e, T, J_E) = \frac{n_{k,j+1}}{n_{k,j}} \simeq \frac{R_{k,j}^{\text{ion}}}{R_{k,j+1}^{\text{rec}}} = \frac{R_{k,j}^{\text{ph}} + n_e(\alpha_{k,j}^{\text{cdi}} + \alpha_{k,j}^{\text{cea}})}{n_e(\beta_{k,j}^{\text{ph}} + \beta_{k,j}^{\text{die}})}. \quad (59)$$

When  $R_{k,j}^{\text{ph}} \ll n_e(\alpha_{k,j}^{\text{cdi}} + \alpha_{k,j}^{\text{cea}})$ , this is the well-known coronal approximation (Dopita & Sutherland 2003), in which the electron density is not required to obtain reasonably accurate number density ratios of adjacent ionization stages.

More generally, however, an estimate of  $n_e$  is required to evaluate Eq. 59. We obtain a zeroth-order approximation for  $n_e$  by solving the transcendental equation of charge conservation (Eq. 57),

$$n_e = \frac{n_{\text{H}}}{\eta_{\text{H}}} \sum_{k=1}^{N_k} \eta_k \sum_{j=1}^{k+1} (j-1) f_{k,j}(n_e, T, J_E). \quad (60)$$

For hydrogen,  $f_{1,1} = 1/(1+\Phi_{1,1})$  and  $f_{1,2} = \Phi_{1,1}f_{1,1}$ , and for helium  $f_{2,1} = 1/(1+\Phi_{2,1}+\Phi_{2,1}\Phi_{2,2})$ ,  $f_{2,2} = \Phi_{2,1}f_{2,1}$ , and  $f_{2,3} = \Phi_{2,2}f_{2,2}$ . In general,  $f_{k,j}$  is computed using a recursive formula. Writing  $f_{k,j} = P_{k,j}/S_k$ , we have

$$P_{k,j} = P_{k,j-1}\Phi_{k,j-1}, \quad S_k = \sum_{j=1}^{k+1} P_{k,j}, \quad (61)$$

where by definition  $P_{k,1} = 1$ . Note that, alternatively,  $f_{k,1} = 1/S_k$  and  $f_{k,j} = \Phi_{k,j-1}f_{k,j-1}$ . Once the zeroth-order  $n_e$  is determined, the zeroth order ionization fractions are known, from which the zeroth-order number densities are computed,

$$n_{k,j} = f_{k,j}n_k = \frac{P_{k,j}}{S_k} \frac{\eta_k}{\eta_{\text{H}}} n_{\text{H}}. \quad (62)$$

#### 8. THE RATE MATRIX

There are  $N = \sum_{k=1}^{N_k} (k+1)$  rate equations (derived in § 6). The equations are closed by the constraint of charge conservation (Eq. 57). If  $n_{\text{tot}}$  was specified instead of  $n_{\text{H}}$ , particle conservation could alternatively be used to close the equations. However, since  $n_{\text{H}}$  constrains the particle densities,  $n_{\text{tot}}$  cannot be determined until after the equilibrium  $n_e$  is determined; thus charge exchange must be employed to close the equations.

Including the charge exchange constraint, the rate matrix comprises  $M = N + 1$  nonlinear equations that must be simultaneously satisfied, i.e., the equilibrium solution is obtained when  $n_{k,j}$  and  $n_e$  yield  $dn_{k,j}/dt = 0$  for all  $k, j$ . This is formalized as the matrix equation  $\mathbf{Mn} = \mathbf{0}$ ,

$$\begin{bmatrix} M_{1,1} & M_{1,2} & 0 & 0 & 0 & 0 \\ M_{2,1} & M_{2,2} & 0 & 0 & 0 & 0 \\ 0 & 0 & M_{3,3} & M_{3,4} & M_{3,5} & 0 \\ 0 & 0 & M_{4,3} & M_{4,4} & M_{4,5} & 0 \\ 0 & 0 & M_{5,3} & M_{5,4} & M_{5,5} & 0 \\ 0 & 1 & 0 & 1 & 2 & -1 \end{bmatrix} \begin{bmatrix} n'_1 (\equiv n_{1,1}) \\ n'_2 (\equiv n_{1,2}) \\ n'_3 (\equiv n_{2,1}) \\ n'_4 (\equiv n_{2,2}) \\ n'_5 (\equiv n_{2,3}) \\ n_e \end{bmatrix} = \begin{bmatrix} 0 \\ 0 \\ 0 \\ 0 \\ 0 \\ 0 \end{bmatrix}, \quad (63)$$

where the example is for a cloud comprising hydrogen and helium only ( $N_k = 2$ ). We denote the row index by  $r$  and the column index by  $c$ . The last row and column close the equations using charge conservation (Eq. 57).

The number densities  $n_{k,j}$  are vectorized to  $n'_r$  and the matrix elements,  $M_{r,c}$ , contain the creation and destruction rates for each  $n'_r$ . The diagonal matrix elements,  $M_{r,r}$ , are the destruction rates for  $n'_r$ , and are thus always negative. For a given row, off-diagonal terms offset by a single column represent the creation of  $n'_r$  via the destruction of an adjacent ionization stage. When metals are included, up to  $j-2$  off-diagonal terms are required for Auger ionization rates.

For a hydrogen and helium gas, the matrix elements are written (compare to § 6),

$$\begin{aligned} M_{1,1} &= - \left( R_{1,1}^{\text{ph}} + n_e \alpha_{1,1}^{\text{cdi}} + \sum_{k=2}^{k+1} \sum_{j=2} n_{k,j} \beta_{k,j-1}^{\text{exH}} \right) \\ M_{1,2} &= n_e \beta_{1,1}^{\text{ph}} + \sum_{k=2}^k \sum_{j=1} n_{k,j} \alpha_{k,j}^{\text{exH}^+} \\ M_{2,1} &= -M_{1,2} \\ M_{2,2} &= -M_{1,1} \\ M_{3,3} &= - \left( R_{2,1}^{\text{ph}} + n_e \alpha_{2,1}^{\text{cdi}} \right. \\ &\quad \left. + n_{1,2} \beta_{1,1}^{\text{exHe}} + \sum_{k=3}^{k+1} \sum_{j=2} n_{k,j} \beta_{k,j-1}^{\text{exHe}} \right) \\ M_{3,4} &= n_e (\beta_{2,1}^{\text{ph}} + \beta_{2,1}^{\text{die}}) \\ M_{3,5} &= 0 \\ M_{4,3} &= -M_{3,3} \\ M_{4,4} &= - (M_{3,4} + M_{5,4}) \\ M_{4,5} &= -M_{5,5} \\ M_{5,3} &= 0 \\ M_{5,4} &= R_{2,2}^{\text{ph}} + n_e \alpha_{2,2}^{\text{cdi}} + n_{1,2} \alpha_{2,2}^{\text{exH}^+} \\ M_{5,5} &= - (n_e \beta_{2,2}^{\text{ph}} + n_{1,1} \beta_{2,2}^{\text{exH}}), \end{aligned} \quad (64)$$

$$M_{3,4} = n_e (\beta_{2,1}^{\text{ph}} + \beta_{2,1}^{\text{die}})$$

$$M_{3,5} = 0$$

$$M_{4,3} = -M_{3,3}$$

$$M_{4,4} = - (M_{3,4} + M_{5,4})$$

$$M_{4,5} = -M_{5,5}$$

$$M_{5,3} = 0$$

$$M_{5,4} = R_{2,2}^{\text{ph}} + n_e \alpha_{2,2}^{\text{cdi}} + n_{1,2} \alpha_{2,2}^{\text{exH}^+}$$

$$M_{5,5} = - (n_e \beta_{2,2}^{\text{ph}} + n_{1,1} \beta_{2,2}^{\text{exH}}),$$

where we have included the charge exchange of metals for purpose of illustration.

#### 9. APPLICATION

In this section, we will show application of the model.

#### 10. CONCLUSIONS

Uhm. Not written, yet.

Thanks to R. Sutherland and to G. Ferland for helpful email exchanges. Much gratitude goes to D. Verner



for providing publicly available electronic tables for photoionization, recombination, collisional ionization, and autoionization and some supporting computational subroutines (<http://www.pa.uky.edu/verner/>). We are grateful for the work of N. Badnell, R. Bingham, G. Duxbury, and H. Summers of the Atomic and Molecular Diagnostic Processes in Plasmas group (<http://amdpp.phys.strath.ac.uk/tamoc/>), who provided radiative and dielectronic recombination rates. We also thank P. Stancil, D. Schultz, J. Wang, M. Raković, J. King-

don, and A. Dalgarno, of the Oakridge National Lab UGA Charge Transfer Database for Astrophysics (<http://www.cfadc.phy.ornl.gov/astro/ps/data/>). CWC was partially support through grant HST-GO-11667.01-A provided by NASA via the Space Telescope Science Institute, which is operated by the Association of Universities for Research in Astronomy, Inc., under NASA contract NAS 5-26555.

## REFERENCES

- Aldrovandi, S. M. V., & Pequignot, D. 1973, *A&A*, 25, 137
- Altun, Z., Yumak, A., Yavuz, I., Badnell, N. R., Loch, S. D., & Pindzola, M. S. 2007, *A&A*, 474, 1051
- Arnaud M., & J. Raymond R. 1992, *ApJ*, 398, 394
- Arnaud, M., & Rothenflug, R. 1985, *A&AS*, 60 425
- Asplund, M., Grevesse, N., Sauval, A. J., & Scott, P. 2009, *ARA&A*, 47, 481
- Badnell, N. R. 1986, *J. Phys. B*, 19, 3827
- Badnell, N. R. 2003, *ApJS*, 167, 334
- Badnell, N. R., O'Mullane, M. G., Summers, H. P., et al. 2003, *A&A*, 406, 1151
- Churchill, C. W., Kacprzak, G. G., Nielsen, N. M., Steidel, C. C., & Murphy, M. T. 2012, *ApJ*, submitted
- Dopita, M. A., & Sutherland, R. S. 2003, *Astrophysics of the Diffuse Universe*, Springer
- Draine, B. T. 2011, *Physics of the Interstellar and Intergalactic Medium*, Princeton University Press, ISBN: 978-0-691-12214-4 (Table 1.4, p8)
- Ferland, G. J., Korista, K. T., & Verner D. A. 1997, *ApJ*, 481, L115
- Ferland, G. J., Hazy, A Brief Introduction to Cloudy 96, University of Kentucky Department of Physics and Astronomy Internal Report
- Haardt, F., & Madau, P. 2011, *ApJ*, arXiv:1105.2039
- Hu, W., Chen, C., Fang, D., Wang, Y., Lu, F., & Yang, F. 1996, *J. Phys. B: At. Opt. Phys.*, 29, 2887
- Kaastra, J. S., & Mewe, R. 1993, *A&AS*, 97, 443
- Kingdon, J. B., & Ferland, G. J. 1996, *ApJS*, 106, 205
- Leitherer, C., Schaerer, D., Goldader, J. D., et al. 1999, *ApJS*, 123, 3
- More, J. J. 1977, in *Numerical Analysis Proceedings*, ed. G. A. Watson, Lecture Notes in Mathematics, 630, Springer-Verlag
- Nussbaumer, H., & Storey, P. J. 1983, *A&A*, 126, 75
- Nussbaumer, H., & Storey, P. J. 1986, *A&AS*, 64, 545
- Nussbaumer, H., & Storey, P. J. 1987, *A&AS*, 69, 123
- Seaton, M. J. 1959, *MNRAS*, 119, 81
- Shull, J. M., & Van Steenberg, M. 1982, *ApJS*, 48, 95
- Verner, D. A., & Iakovlev, D. G. 1990, *Ap&SS*, 165, 27
- Verner, D. A., & Iakovlev, D. G. 1995, *A&AS*, 109, 125
- Verner, D. A., Ferland, G. J., Korista, K. T., & Iakovlev, D. G. 1996, *ApJ*, 465, 487
- Voronov, G. S. 1997, *Atomic Data and Nuclear Data Tables*, 65, 1